Hydrogen isotopes in high ^{3}He/^{4}He submarine basalts: Primordial vs. recycled water and the veil of mantle enrichment

Matthew W. Loewen [a,c,*], David W. Graham [b], Ilya N. Bindeman [c], John E. Lupton [d], Michael O. Garcia [e]

[a] *Alaska Volcano Observatory, U.S. Geological Survey, Anchorage, AK 99508, United States of America*
[b] *College of Earth, Ocean, and Atmospheric Sciences, Oregon State University, Corvallis, OR 97331, United States of America*
[c] *Department of Earth Sciences, University of Oregon, Eugene, OR 97403, United States of America*
[d] *NOAA Pacific Marine Environmental Laboratory, Newport, OR 97365, United States of America*
[e] *Department of Geology & Geophysics, SOEST, University of Hawaii, Honolulu, HI 96822, United States of America*

ARTICLE INFO

ABSTRACT

The hydrogen isotope value (δD) of water indigenous to the mantle is masked by the early degassing and recycling of surface water through Earth's history. High ^{3}He/^{4}He ratios in some ocean island basalts, however, provide a clear geochemical signature of deep, primordial mantle that has been isolated within the Earth's interior from melting, degassing, and convective mixing with the upper mantle. Hydrogen isotopes were measured in high ^{3}He/^{4}He submarine basalt glasses from the Southeast Indian Ridge (SEIR) at the Amsterdam–St. Paul (ASP) Plateau (δD = −51 to −90‰, ^{3}He/^{4}He = 7.6 to 14.1 R_A) and in submarine glasses from Loihi seamount south of the island of Hawaii (δD = −70 to −90‰, ^{3}He/^{4}He = 22.5 to 27.8 R_A). These results highlight two contrasting patterns of δD for high ^{3}He/^{4}He lavas: one trend toward high δD of approximately −50‰, and another converging at δD = −75‰. These same patterns are evident in a global compilation of previously reported δD and ^{3}He/^{4}He results. We suggest that the high δD values result from water recycled during subduction that is carried into the source region of mantle plumes at the core–mantle boundary where it is mixed with primordial mantle, resulting in high δD and moderately high ^{3}He/^{4}He. Conversely, lower δD values of −75‰, in basalts from Loihi seamount and also trace element depleted mid-ocean ridge basalts, imply a primordial Earth hydrogen isotopic value of −75‰ or lower. δD values down to −100‰ also occur in the most trace element-depleted mid-ocean ridge basalts, typically in association with ^{87}Sr/^{86}Sr ratios near 0.703. These lower δD values may be a result of multi-stage melting history of the upper mantle where minor D/H fractionation could be associated with hydrogen retention in nominally anhydrous residual minerals. Collectively, the predominance of δD around −75‰ in the majority of mid-ocean ridge basalts and in high ^{3}He/^{4}He Loihi basalts is consistent with an origin of water on Earth that was dominated by accretion of chondritic material.

Published by Elsevier B.V.

1. Introduction

Water on the Earth's surface is essential for the development of life. In the mantle it contributes to partial melting and rheological behavior during solid state convection (e.g., McGovern and Schubert, 1989; Hirschman, 2006). Despite this first-order importance for planetary evolution, a basic question remains regarding how much water in mantle-derived magmas is juvenile, i.e., primordial water that has never been present at Earth's surface (representing original accreted planetary water), versus water from recycling by subduction throughout Earth's history (e.g., Lécuyer et al., 1998; Hirschmann, 2006; Marty, 2012; Parai and Mukhopadhyay, 2012; Peslier et al., 2017). This question may be addressed by coupling measurements in mantle-derived materials of water and its isotopic composition with other indicators of mantle provenance. The deuterium/hydrogen ratio is the most diagnostic, and is expressed in delta notation relative to standard mean ocean water as δD = {(D/H)$_{sample}$/(D/H)$_{SMOW}$ − 1} × 10^3.

High ^{3}He/^{4}He ratios associated with ocean island basalt (OIB) volcanism track the presence of primitive mantle that has been isolated from melting and degassing since the earliest stages of
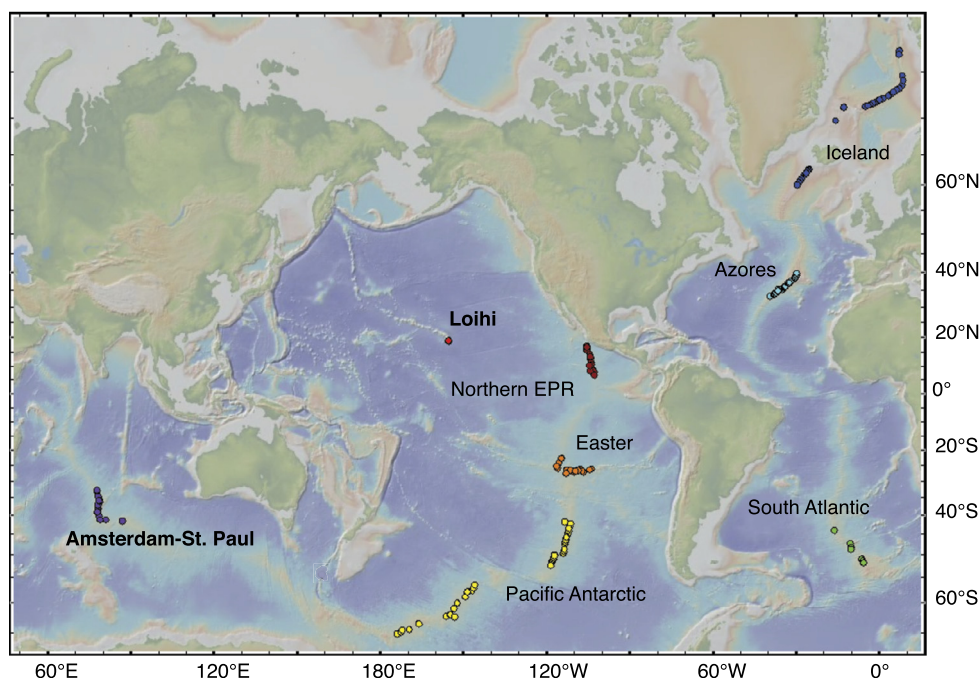
Fig. 1. Map showing the distribution of submarine basalt glasses from mid-ocean ridges and ocean islands analyzed for δD. New analyses are from the Amsterdam–St. Paul Plateau and Southeast Indian Ridge, and from Loihi seamount on the flank of Hawaii. Previous δD analyses by identical methods to this study (TC/EA, University of Oregon)—from the Northern East Pacific Rise (EPR), Azores, and Easter—are reported in Dixon et al. (2017). Other δD analyses measured with conventional manometry are included for Easter, Iceland, and the South Atlantic by Dixon et al. (2017), and for the Pacific–Antarctic Ridge by Clog et al. (2013).

Earth history (e.g., Allègre et al., 1983; Mukhopadhyay, 2012). Only a few studies have directly compared δD measurements with ^{3}He/^{4}He, despite the fact that both hydrogen and helium should be incompatible during mantle melting (Aubuad et al., 2004; Graham et al., 2016), therefore making high ^{3}He/^{4}He samples a prime target for understanding primordial hydrogen isotopic values (Craig and Lupton, 1976; Rison and Craig, 1983; Poreda et al., 1986). These earlier studies, however, found that a high ^{3}He/^{4}He signature is variably coupled with tracers of mantle enrichment, such as isotopes of Sr–Nd–Pb, that represent the time integrated history of mantle melting and subduction recycling. These co-variations suggest that recycled and primordial material can be admixed in the mantle (e.g., Kurz et al., 1982; Hanan and Graham, 1996), and this has prevented an unambiguous characterization of primordial hydrogen isotope values.

The early study by Poreda et al. (1986) of basalts from the Reykjanes, Kolbeinsey, and Mohns Ridges around Iceland showed that δD was best correlated with trace element indicators of mantle enrichment such as La/Sm, and also with total water concentrations. Trace element ratios and water concentrations can reflect both the character of the mantle source and/or the degree of partial melting. The results for ^{3}He/^{4}He and δD showed diverging trends, to both high and low δD ($-50\textperthousand$ and $-90\textperthousand$) in the highest ^{3}He/^{4}He samples from the Reykjanes Ridge. Ultimately, Poreda et al. (1986) could not determine whether the high δD values in high ^{3}He/^{4}He basalts indicated a stronger component of primordial water vs. water derived from recycled lithosphere/crust. A stronger relationship of high δD and high ^{3}He/^{4}He is present for basalts from the Easter Island hotspot region of the East Pacific Rise (data from Poreda et al., 1993; Kingsley et al., 2002). However, those results also do not resolve if the δD values were primarily influenced by recycled or primordial water, or both.

The recent comprehensive study of water and D/H in global mid-ocean ridge basalts (MORB) by Dixon et al. (2017) indicates the presence of a diversity of enriched components. Dixon et al. (2017) proposed that many subducting slabs undergo a primary phase of dehydration, followed by a secondary phase of rehydra-

tion due to the release of water from alteration minerals within cooler parts of the slabs at greater depths. Slab temperature is a key variable in the Dixon et al. (2017) model, and it largely dictates the degree of coupling between H_2O and lithophile element tracers. According to this model, the entire global range of mantle δD is a result of differences in the evolution of hot vs. cold slabs during subduction. Dixon et al. (2017) concluded that interaction with primordial material might occur during slab recycling to the deep mantle, but they did not investigate co-variations between δD and ^{3}He/^{4}He.

Defining Earth's primordial δD has been elusive, with values proposed as extreme as $\delta D = -218\textperthousand$ (Hallis et al., 2015) to values of -60 to $-80\textperthousand$ that are more typical of MORB (Lécuyer et al., 1998). The more traditional MORB-like value for primordial δD in Earth matches average meteoritic δD values and has been taken as support for a chondritic origin of Earth's water (Marty and Yokochi, 2006). In contrast, the much lower δD value suggested from melt inclusion studies of high ^{3}He/^{4}He basalts from Baffin Island (Hallis et al., 2015) may point to trapped water from solar nebula gas during accretion. However, the accurate determination of δD values and water concentrations in melt inclusions are difficult and can be problematic (e.g., Hauri, 2002; Portnyagin et al., 2008; Gaetani et al., 2012), and questions remain about how to best interpret very low δD values for Baffin melt inclusions (Michael, 2017; Gatti et al., 2018). An improved characterization of δD variations in high ^{3}He/^{4}He submarine glasses is needed to understand the primordial δD composition of the Earth.

Advances in continuous flow mass spectrometry (Sharp et al., 2001; Bindeman et al., 2012; Martin et al., 2017) allow analyzing D/H ratios and water concentrations on milligram quantities of water-poor glass, which is 100 times less material than by conventional methods. This permits analysis of the purest glass concentrate. In this study we utilized these methods to analyze submarine glasses from localities with high ^{3}He/^{4}He basalt: the Southeast Indian Ridge (SEIR) in the vicinity of the Amsterdam–St. Paul (ASP) Plateau and Loihi seamount south of the island of Hawaii (Fig. 1). Both localities represent the surface manifestation

of a mantle plume and have ^{3}He/^{4}He that extends well above the values typically found in upper mantle-derived basalts; ^{3}He/^{4}He in some Loihi seamount lavas are among the highest measured at ocean islands. These localities are also well characterized in their trace element and Sr–Nd–Pb isotopic compositions, but they have not been investigated in detail for D/H ratios. These new results are synthesized with previous analyses of δD and ^{3}He/^{4}He in oceanic basalts worldwide (Fig. 1; Dixon et al., 2017). Collectively these data sets provide a more robust framework to evaluate the hydrogen isotopic composition of the deep mantle and the potential contributions of primordial water and recycled water to ocean ridge and mantle plume basalts.

2. Samples and methods

2.1. Sample selection

The SEIR crosses the ASP Plateau in the southern Indian Ocean. The plateau contains numerous seamounts and the two islands of Amsterdam and St. Paul, which lie approximately 60 and 100 km, respectively, from the nearby spreading ridge. Submarine basalts from the SEIR atop the plateau, and from the areas to the northwest and the southeast of the plateau, have been recovered at roughly 10–15 km spacing. These basalts are well characterized for major elements and He–Sr–Nd–Pb isotopes (Douglas-Priebe, 1998; Graham et al., 1999; Johnson et al., 2000; Nicolaysen et al., 2007). Notably for our study, ^{3}He/^{4}He values are elevated, up to 14 R$_A$ (where R$_A$ is the atmospheric ^{3}He/^{4}He ratio), on the ASP plateau and along the spreading the ridge segment (H) immediately to its northwest.

Submarine glasses were analyzed for δD and H$_2$O from 18 dredge and wax core locations along the SEIR, collected by the R/V *Melville* during the Boomerang 06 expedition. Samples selected for this study contain 0.1 to 1 wt.% water and were all collected at water depths greater than 1500 m ($>$15 MPa). At these depths, water concentrations up to 1.25 wt.% should remain saturated in a basaltic melt (Newman and Lowenstern, 2002). Trace element data for these samples have been obtained by Laser Ablation-Inductively Coupled Plasma-Mass Spectrometry (LA-ICP-MS) using methods similar to those described in Michael and Graham (2015) and Loewen and Kent (2012) and are reported in Table S1.

Loihi seamount is the youngest expression of active volcanism associated with the Hawaiian hotspot (Moore et al., 1982). It lies about 35 km south of Hawaii and is constructed on the submarine flanks of Mauna Loa and Kīlauea. Loihi lavas show limited Sr–Nd–Pb isotopic variability with no correlation with degree of silica saturation or age; thus the range in rock compositions is thought to be derived by variable degree of melting of a common mantle source (Garcia et al., 1989, 1993, 1998). ^{3}He/^{4}He values of Loihi basalts range to values $>$30 R$_A$ (Kurz et al., 1983; Rison and Craig, 1983).

Thirteen submarine basalt glasses were analyzed from Loihi seamount. These samples were collected in 1983 by dredges from the R/V *Kana Keoki*, in 1987 by the *Alvin* submersible during dives 1801–1804, and in 1996 by the *Pisces V* submersible during dive 286 following the 1996 Loihi summit eruption. Major, trace, volatile, and isotopic data for these samples are reported in Garcia et al. (1989, 1993, 1998), and Pietruszka et al. (2011). Rock types analyzed include tholeiitic, transitional, and alkali basalts. The Loihi samples were erupted at shallower depths (1000–1350 m) than the analyzed SEIR glasses, and hence we critically assess the potential degassing effects for that sample suite.

2.2. Hydrogen isotope analyses

Determinations of δD and total water concentrations were made by a Thermal Conversion Elemental Analyzer (TC/EA) cou-

pled to a MAT 253 10 kV gas source isotope ratio mass spectrometer (IRMS) at the University of Oregon (Bindeman et al., 2012; Martin et al., 2017). Clean, unaltered glass was crushed and sieved to the 250–50 μm size fraction and visually inspected to ensure purity of the glass separate, 5–10 mg wrapped into silver capsules, heated in a $\sim$150 °C vacuum overnight to remove adsorbed water, and loaded into a He-purged autosampler. Samples were run in 2–6 replicates. All individual sample analyses are reported in Table S2. Values of δD used for plotting, and for comparison between samples, are the medians of these replicate analyses. The median limits the influence of an occasional disparate measurement more effectively than the mean.

Multiple standards were analyzed concurrently with the unknown glasses during each analytical session, including direct standard waters welded in silver cups: VSMOW (0‰), W62001 (−41.5‰), and Lake Louise (−150.2‰) produced by the U.S. Geological Survey (Qi et al., 2010). Solid standards included in-house micas: NBS30 (−50.0‰), RUH2 (−81.4‰), BUD (−144.7‰), as well as recently calibrated mica standards USGS57 (−91‰), and USGS58 (−28‰) (Qi et al., 2017). We note that our nominal value of NBS30 is 16‰ higher than the −65.7‰ reference value used in the majority of historical studies (see Martin et al., 2017 for discussion). Our offset is a result of direct measurement of NBS30 relative to water standards in our TC/EA system and a now recognized offset between TC/EA and conventional δD determinations (Qi et al., 2014, 2017); this offset is likely a result of heterogeneity in NBS30 splits related to grain size variations (see Martin et al., 2017 and Qi et al., 2017 for a detailed discussion). We caution against directly comparing these results to studies that rely on NBS30 as a reference standard without correcting for heterogeneity of any particular split of standard.

For analytical sessions utilized in this dataset, the 2σ reproducibility for NBS30 = 5.5‰ ($n = 19$ excluding a single $>3\sigma$ outlier), RUH2 = 3.0‰ ($n = 16$), and BUD = 6.0‰ ($n = 19$). The average range of replicate analyses for individual samples is 5‰, although some Loihi samples had a range of values in replicate analyses of up to 20‰. We suggest this larger range is indicative of sample heterogeneity due to hydrogen isotope fractionation during loss of small amounts of H$_2$O by degassing (see section 3.2 for more discussion). Median values were used for each sample to reduce the effects of sample heterogeneity.

We focus on comparing our new δD data to previously published TC/EA data, due to systematic offsets that may exist between TC/EA and other methods. Dixon et al. (2017) described a $\sim$10‰ systematic offset between 6 samples measured by both TC/EA and conventional stepped-heating manometry. Clog et al. (2012) also observed similar offsets between different conventional techniques. It is currently unclear which method provides a more accurate measurement of δD, and there are insufficient replicate data to provide an accurate interlaboratory correction.

Total water concentrations were determined by peak integration during the TC/EA analyses, using a nominal 3.5 wt.% in the NBS30 biotite mica standard. Rapid thermal pyrolysis of hydrous glasses by TC/EA at 1450°C releases 100% of water in glass. This is established by comparison to independently determined (by FTIR or manometry) water concentrations for the same aliquots of basalt glasses in a wide range of H$_2$O from 0.1 to 1.2 wt.%, including water-poor glasses having $<$0.5 wt.% H$_2$O (Bindeman et al., 2012; Martin et al., 2017; Dixon et al., 2017).

2.3. Helium isotope analyses

Helium isotope results for the SEIR sample suite were reported previously (Graham et al., 1999; Nicolaysen et al., 2007). Table S3 provides results for 11 new He analyses from Loihi seamount along with 2 previously reported values (samples 286-1 and 286-5) from

Garcia et al. (1998). All basalt glasses from Loihi were analyzed at NOAA/PMEL in Newport, Oregon, following methods outlined in Graham et al. (1999). Samples were lightly crushed and 1–5 mm-sized chunks of fresh glass free of alteration were selected using a binocular microscope. The selected glass was cleaned ultrasonically in deionized water and acetone and air dried. Sample weights ranged between 280 and 475 mg. The selected glass samples were crushed on-line to release the gas trapped in vesicles for He isotope analysis. Sample powders retrieved from the crushers were transferred to a high temperature vacuum furnace to also measure [He] and ^{3}He/^{4}He dissolved in the glass. The crushed powders were transferred to Al-foil boats, dropped into the furnace crucible and melted at 1400 °C. Processing line blanks were analyzed before each sample and ranged from ∼2 to 4 × 10^{-10} cm^3 STP ^{4}He. The He concentration and isotope value of samples were calibrated against aliquots of known size of marine air collected in Newport. Aliquots of a geothermal gas secondary standard, collected from Yellowstone Park (MM = Murdering Mudpots, having ^{3}He/^{4}He = 16.5 R$_A$), were also analyzed routinely to correct for small (<3%) mass discrimination effects related to variations in gas pressure in the mass spectrometer.

3. Results and discussion

3.1. Southeast Indian Ridge

δD varies along the SEIR between −90‰ and −51‰, covering much of the range of δD reported globally for oceanic basalts (Kyser and O'Neil, 1984; Poreda et al., 1986; Kingsley et al., 2002; Dixon et al., 2017). Higher δD values are generally associated with geochemically enriched samples in the ASP Plateau region (Fig. 2). The strongest co-variations involving δD are with incompatible species (e.g., water, K$_2$O, La), and with ratios of highly incompatible/moderately incompatible elements (e.g., La/Sm, K/Ti; see Fig. S1). These ratios and concentrations can reflect either enriched incompatible element concentrations in the source region or low degrees of partial melting, or both. The highest δD values (DR64-2, WC37 and WC47) tend to be associated with the radiogenic ^{206}Pb/^{204}Pb signature of the ASP mantle plume and are found throughout the plume influenced region (on ridge segments I, J, and H; Fig. 2). This plume Pb isotopic composition is identical to the common (C)-type composition described by Hanan and Graham (1996) in their treatment of global MORB and OIB data sets. The most enriched SEIR lavas having this signature are erupted along segment H, located immediately northwest of the ASP Plateau (Fig. 1). Segment H is also characterized by very large He–Pb–Sr–Nd isotopic diversity (Graham et al., 1999; Nicolaysen et al., 2007). The new results presented here show that this diversity also characterizes hydrogen isotopes. For example, there is a systematic decrease in δD of segment H lavas, from enriched (e.g., high La/Sm; WC47, δD = −53‰) to depleted basalts (e.g., low La/Sm; DR73-6, δD = −79‰). Some lavas atop the ASP Plateau (on segments I and J) have a distinct isotope composition characterized by markedly higher ^{87}Sr/^{86}Sr and ^{208}Pb/^{206}Pb (Figs. S1, S2), referred to as Dupal-type (Hart, 1984), possibly a reflection of recycled lower continental crust or lithosphere (e.g., White, 2015). These Dupal-type basalts do not all seem to exhibit high δD values (e.g., DR59-1, δD = −76‰; Fig. 2).

The high δD values in ASP basalts are a signature of their mantle source, and do not result from secondary processes such as (1) shallow degassing, (2) seawater contamination, or (3) magma evolution/crystal fractionation as discussed below.

Our observations exclude shallow degassing and any associated H$_2$O loss as a significant process in producing the observed δD variations. Degassing will lower the δD value of a residual melt, as D will be concentrated in the vapor phase molecular water (e.g.,
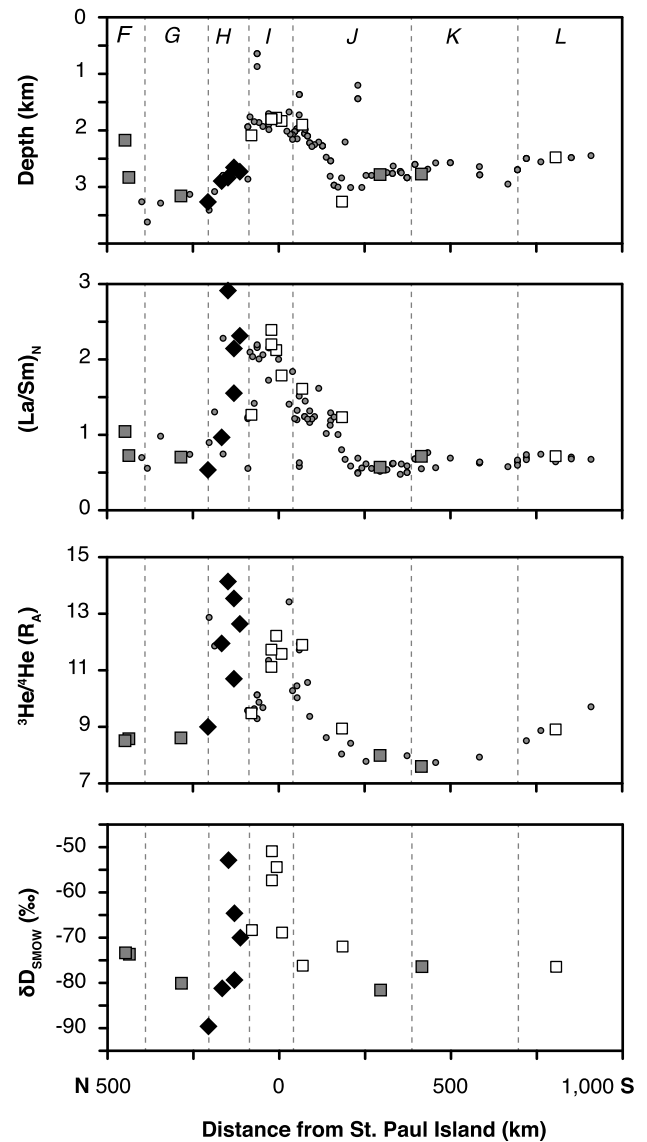
Fig. 2. Variations in axial depth (km), chondrite-normalized La/Sm, ^{3}He/^{4}He (R$_A$) and δD$_{SMOW}$ (‰) vs. along-axis distance (km) for submarine basalts from the Southeast Indian Ridge in the vicinity of the Amsterdam–St. Paul Plateau (ASP). Divisions between the different ridge segments F through L are shown by vertical dashed lines. Filled gray squares and all segment H diamonds designate samples with MgO > 7.5 wt.%, outlined squares have MgO < 7.5 wt.%. Small circles designate other samples that were not analyzed for δD. The geochemical anomaly associated with the shallower ridge axis atop the plateau (segments I, J) are also found in segment H (diamonds) ∼100 km to the northeast in an area with no depth anomaly. Helium isotope data are from Nicolaysen et al. (2007) and Graham et al. (1999).

Hauri, 2002; De Hoog et al., 2009). In our analyzed basalts, samples with the highest water concentrations, and therefore having the potential for larger amounts of water loss accompanying the degassing of CO$_2$-saturated melts (Fig. 3A), actually have the highest δD values. This is the opposite to the expectation that residual water in partially degassed melts will have lower δD (Fig. 3B).

Seawater contamination can be examined in submarine glasses with measurements of Cl (Fig. 4). Two samples from segment I atop the ASP Plateau have elevated [Cl] and excess Cl (Cl that results from seawater or brine assimilation, as opposed to mantle melting or crystal fractionation processes. Excess Cl is computed from the relation between Cl/K and K/Ti; see Michael and Cornell, 1998). Segment H basalts that do not have elevated Cl contents or Cl/K ratios, however, have similar δD values. Also, MORB glasses having high Cl or Cl/K do not typically show anomalously high δD
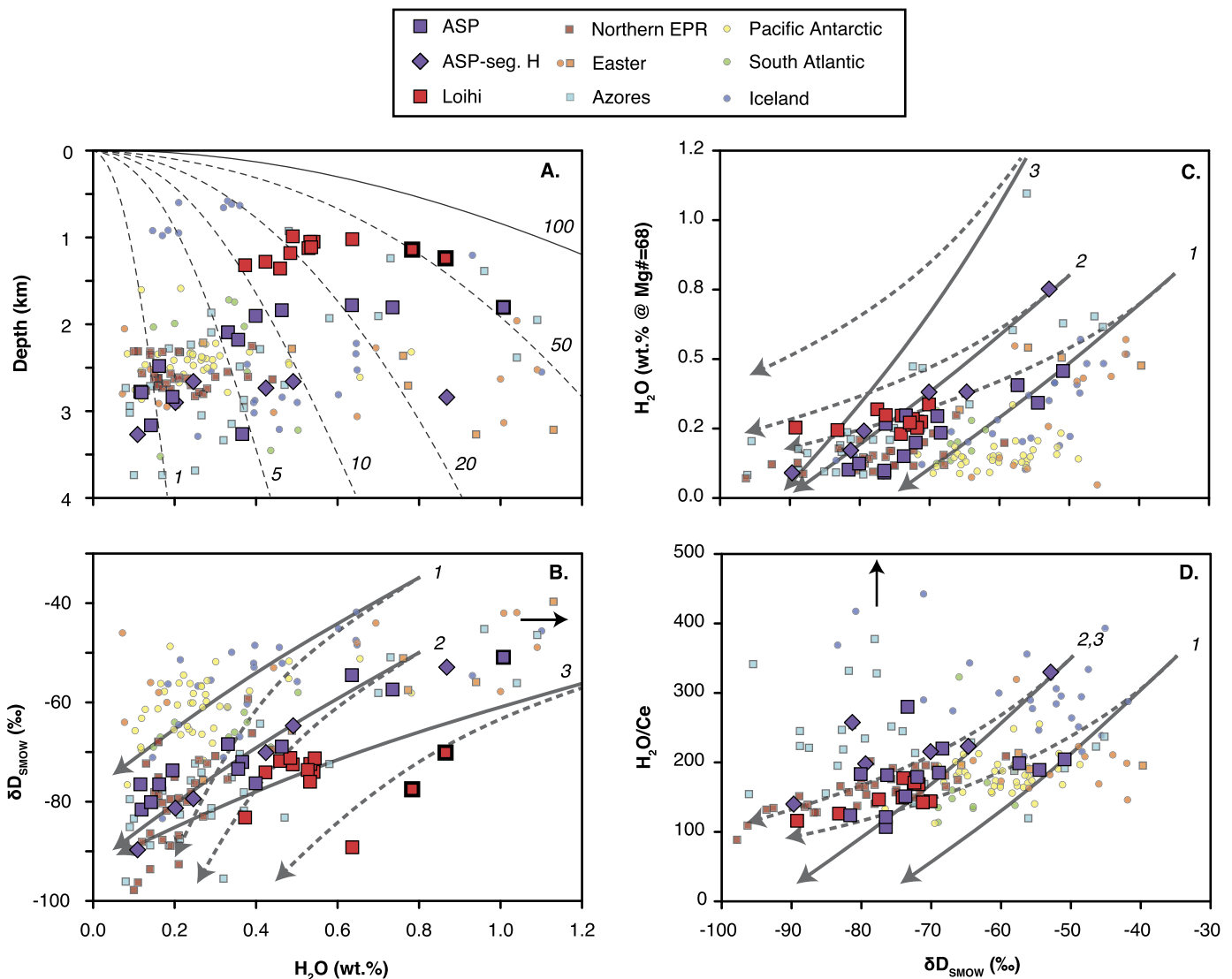
Fig. 3. Sample water concentrations compared to (**A**) depth of sample recovery at the seafloor, and (**B**) δD. Sample δD compared to (**C**) water concentrations corrected for crystal fractionation, and (**D**) H_2O/Ce. Solid line in (**A**) corresponds to vapor saturation of H_2O in a basaltic melt at 1200 °C, while dashed lines show variations in the molar % H_2O with depth for a H_2O–CO_2 equilibrium saturated fluid (calculated in VolatileCalc, Newman and Lowenstern, 2002). In (**B**), lines correspond to the hydrogen isotope shift during closed-system (solid) vs. open-system (dashed) degassing for three different initial conditions: 0.8 wt.% H_2O and −35‰ (1) or −50‰ (2), and 1.5 wt.% H_2O and −50‰ (3). The calculated vapor-melt fractionation follows the model of De Hoog et al. (2009) for a basaltic magma. The three samples from this study that lie closest to saturation are highlighted in a thicker black outline. Each of these samples lie near the highest H_2O and δD for their respective sample suites, so degassing cannot explain their relative positions. The same degassing curves are shown in (**C**) for the water concentrations corrected for crystal fractionation to primary melt values of $Mg\# = 68$, following Michael and Graham (2015), and in (**D**) against H_2O/Ce, which is expected to be constant with different degrees of crystal fractionation and partial melting. Arrows in (**B**) and (**D**) denote some samples from Iceland and Easter datasets excluded due to unusually high water and/or H_2O/Ce. Note that for previously published δD data (in Clog et al., 2013; Dixon et al., 2018), samples shown as squares were measured by TC/EA, directly comparable to this work, and samples shown as circles were measured by conventional methods. (For interpretation of the colors in the figure(s), the reader is referred to the web version of this article.)

as might be expected from seawater assimilation (Figs. 4 and S1; Kingsley et al., 2002; Clog et al., 2013). This observation suggests that the process responsible for the elevated Cl in most ocean ridge basalts may be assimilation of halite that has minimal water content and high Cl (e.g., Michael and Cornell, 1998; Kent et al., 1999; Pietruszka et al., 2011), and thus has little effect on δD values.

Crystal fractionation of non-hydrous minerals should not fractionate hydrogen isotopes and therefore crystal fractionation during magma evolution in the crust cannot be responsible for the observed δD variations in the SEIR basalts. Although some fractionated low MgO (<7.5 wt.%) basalts have relatively high δD values, elevated δD values are also found in high MgO basalts from segment H (Fig. 2), supporting this contention.

Finally, we also note that the lowest δD value in the SEIR basalt suite occurs in the most trace element depleted MORB glass

(DR75-1, $\delta D = -90$‰) that was collected from a short relay zone within the Zeewolf Transform between segments H and G.

3.2. Loihi seamount

The Loihi glass samples show a narrow range of $^3He/^4He$ for the gas trapped in vesicles (21.4–27.8 R_A) that is released by crushing in vacuum (one sample, ALV1803-14, is an exception: it has of a very low [He] $<2 \times 10^{-9}$ cm^3 STP/g and $^3He/^4He$ < 14 R_A). The range of $^3He/^4He$ in samples analyzed here overlaps previously reported values from Loihi (e.g., Kurz et al., 1983; Rison and Craig, 1983; Honda et al., 1993). These values are among the highest measured $^3He/^4He$ ratios in submarine basalt glasses from plume-derived ocean island localities. Melting of the powders retrieved after the crushing analyses revealed a larger range of $^3He/^4He$ (10.3–26.3 R_A) in the glass that extends to lower
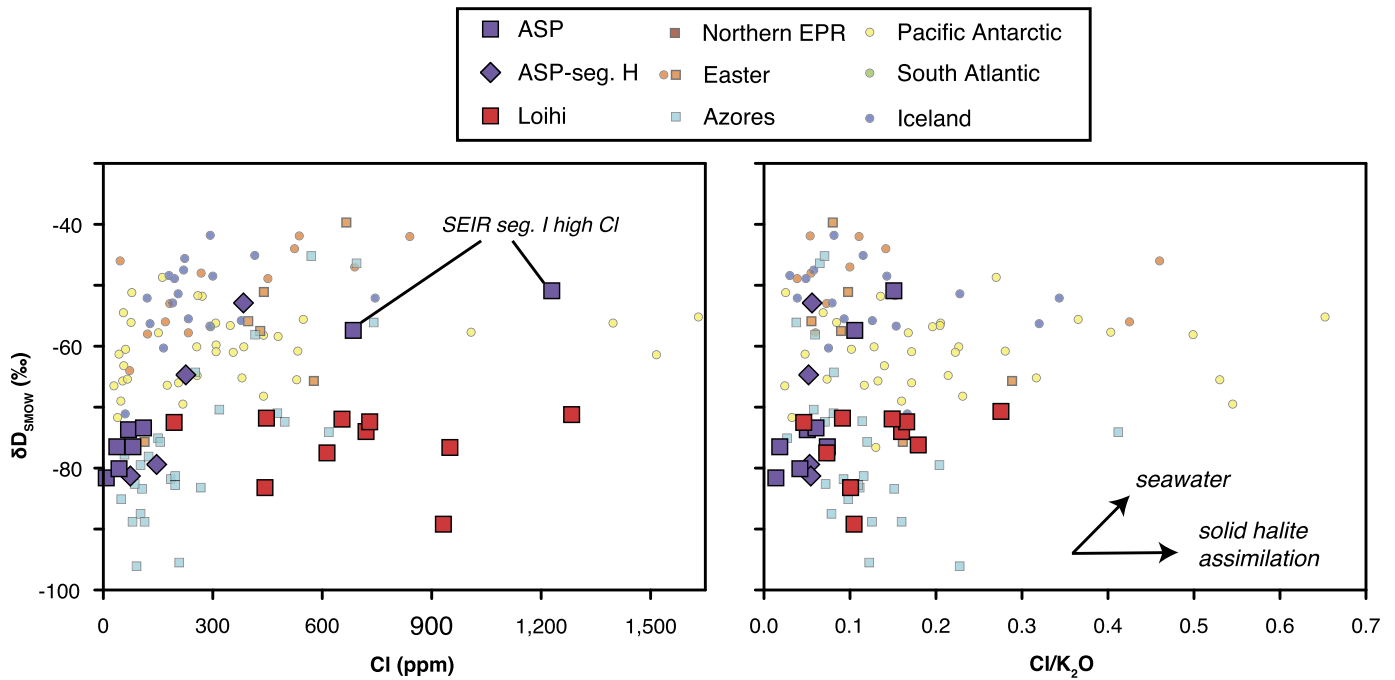
Fig. 4. δD vs. [Cl] and Cl/K$_2$O in suites of submarine basalts distributed globally. [Cl] broadly covaries with δD in the ASP sample suite; however, globally there is no clear trend. Cl/K$_2$O shows no clear trends. Assimilation or contamination by seawater would result a trend toward δD = 0‰. The relatively flat trend to high Cl/K$_2$O instead suggests possible interaction with a highly saline brine or solid halite for the most Cl-enriched basalts. Symbols are the same as Fig. 3.

values than observed in the vesicles. Three samples show a significant amount He isotope disequilibrium between vesicles and glass (1802-4B, 1803-14, 1804-19); these samples have the lowest amount of He dissolved in the glass phase. This suggests that at these low dissolved He concentrations we can detect ingrowth of post-eruptive radiogenic ^{4}He (Graham et al., 1987). We calculated ages of 2.0 to 7.3 kyr for these three samples given their measured He isotope disequilibrium and reported U and Th concentrations (see Supplementary Material and Table S3 for further discussion). Other Loihi basalts have similar vesicle and melt ^{3}He/^{4}He, so estimates of their eruption ages are not possible from the He isotope disequilibrium method.

The Loihi basalts are relatively evolved magmas (MgO = 5–8 wt.%) and less compositionally diverse than the ASP suite. They were erupted at relatively shallow water depths (950–1350 m). Nonetheless, even at this pressure, the measured water concentrations of <1 wt.% should be water-undersaturated (Fig. 3A). Like the ASP sample suite, only samples with the highest water concentrations could undergo any water loss during degassing of a CO$_2$-saturated melt, yet those samples do not have δD values that are lower than other Loihi samples (Figs. 3A, B).

Estimates of the water concentrations for a parental magma having Mg# (molecular Mg/Mg + 0.9 ∗ Fe) = 68 results in a tight cluster of all but two of the Loihi basalts (Fig. 3C). For all but these two samples, there is a narrow range of δD from −70‰ to −78‰, and a small range of H$_2$O/Ce from 142 to 177 (Fig. 3D). These δD values are significantly lower than those of the ASP samples having high ^{3}He/^{4}He (where δD extends to −50‰). The δD values of −70‰ to −78‰ correspond closely to previous estimates for Hawaii and Loihi (Friedman, 1967; Rison and Craig, 1983; Garcia et al., 1989) and fall in a more restricted range than the δD results from melt inclusions (−79‰ to −118‰ at Loihi, +40‰ to −165‰ at other Hawaiian volcanos, Hauri, 2002). The H$_2$O/Ce values are also identical to the Loihi value of 167 ± 13 reported by Dixon and Clague (2001).

Two Loihi basalts have lower δD values of −83‰ and −89‰ and significantly lower H$_2$O/Ce = 120. These samples also have the

highest vesicularity for the Loihi suite ($\sim$40 vol.%; Table S3). Their high vesicularity, along with their relatively shallow eruption pressures, suggests that some hydrogen isotope fractionation occurred during the small amount of water loss that would have accompanied their extensive CO$_2$ degassing (e.g., De Hoog et al., 2009; Fig. 3B). This may have occurred under equilibrium degassing conditions, or it may be a disequilibrium phenomenon. Dixon and Clague (2001) noted that disequilibrium between molecular [H$_2$O] and [OH$^-$] in Loihi glasses is consistent with small amounts of water diffusion into vesicles. This process might account for the low δD and H$_2$O/Ce in these two anomalous samples, as well as the greater range of δD in replicate analyses of other Loihi samples.

3.3. Global δD variability in submarine basalts

Our new δD values for the SEIR basalts and for Loihi seamount provide two contrasting patterns of water and δD behavior in two different high ^{3}He/^{4}He sample suites. We consider the implications of these two patterns within a broader global context, using published δD–^{3}He/^{4}He that includes the large compilation of δD values from globally distributed submarine basalts reported in Dixon et al. (2017). Samples from the Azores Platform (North Atlantic), northern East Pacific Rise (EPR) near the Orozco Fracture Zone, and a subset of those from the Easter Microplate and Easter-Salas y Gomez seamounts were measured by the same TC/EA laboratory and procedure as the ASP and Loihi samples studied here. We also consider *trends* of conventional δD results from the Mid-Atlantic Ridge north and south of Iceland (Poreda et al., 1986), the Easter Microplate and Easter-Salas y Gomez seamounts (Poreda et al., 1993; Kingsley et al., 2002; revised in Dixon et al., 2017), the Pacific Antarctic Ridge (Clog et al., 2013), and the South Atlantic Discovery and Shona geochemical anomalies (Dixon et al., 2017). As discussed in section 2.2, these conventional δD data may be systematically offset from TC/EA measurements.

The overall global compilation of submarine glass δD values measured by TC/EA shows a normal distribution ranging from −98‰ to −40‰, with a mean of −75‰ (1σ = 12‰, n = 95;
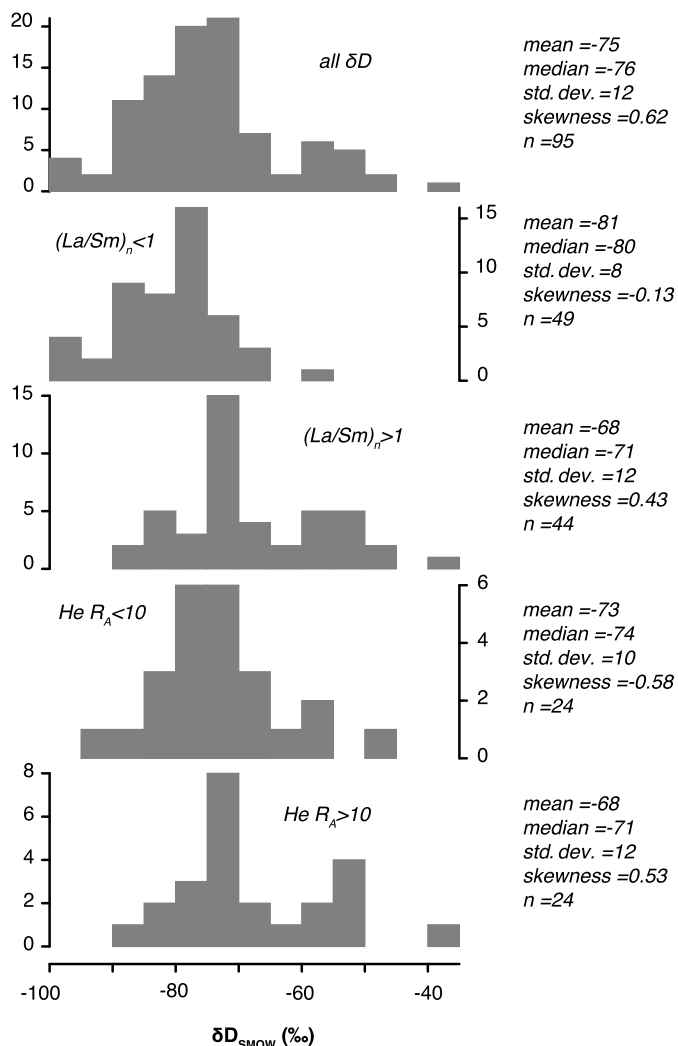
Fig. 5. Frequency distribution of δD values measured in submarine glasses by TC/EA. Data are from this study and Dixon et al. (2017). The δD results are normally distributed, with 50% of the samples lying between -65 and $-80‰$. Depleted mantle samples with $(La/Sm)_n < 1$, have a similar normal distribution but are offset to lower δD with no values greater than $-55‰$. Samples with enriched mantle signatures, $(La/Sm)_n > 1$, resemble a bimodal distribution having one proportion of the population offset to δD near -50 to -60, and some values as high as $-40‰$. Similar distributions are observed for the more limited subset of samples with measured $^3He/^4He$ ratios. Typical MORB mantle samples having $^3He/^4He < 10\ R_A$ show a normal distribution with a peak around -70%, while samples having elevated $^3He/^4He > 10\ R_A$ show a bimodal pattern.

Fig. 5). Basalts derived from nominally depleted mantle, defined as those having chondrite-normalized $(La/Sm)_n < 1$, have a pattern similar to the overall data set, but their upper limit is $-59‰$ ($\bar{x} = -81‰$, $n = 49$). In contrast, enriched mantle basalts with $(La/Sm)_n > 1$ display a pattern resembling a bimodal distribution, with one peak at -70 to $-75‰$, similar to the overall data set, and another peak at -50 to $-60‰$ (overall $\bar{x} = -68‰$, $n = 44$). The δD distributions using $^3He/^4He$ as a discriminant are similar to those based on mantle enrichment. We have chosen 10 R_A as a cutoff value for an approximate upper limit in basalts derived from the depleted mantle (Graham et al., 2014). Basalts having $^3He/^4He < 10\ R_A$ are normally distributed with a mean of $-73‰$ ($n = 24$), and basalts with $^3He/^4He > 10\ R_A$ show two peaks at -70 to $-75‰$ and -50 to $-55‰$ (overall $\bar{x} = -68‰$, $n = 24$).

Both the SEIR basalt suite and the global submarine data set show that δD is broadly correlated with mantle enrichment factors such as La/Sm, and with long-lived isotopic tracers of enrichment

such as $^{206}Pb/^{204}Pb$ and $^{87}Sr/^{86}Sr$ (Figs. 6, 7, S2). There is considerable scatter as expected when including basalts from many different regions, and some extreme samples lying away from the broad trends are also found (e.g., the highest $^{87}Sr/^{86}Sr$ basalts from the South Atlantic and the ASP region of the SEIR; Fig. 7). Some individual sample groups show a strong covariation, such as segment H from the SEIR, where δD, La/Sm, and $^{206}Pb/^{204}Pb$ encompass ~75% of the global range along mid-ocean ridges (Figs. 2, S1, S2).

No global pattern toward higher δD values at high $^3He/^4He$ ratios is observed (Fig. 6). Although positive correlations are found within individual sample suites (e.g., ASP, Easter), basalt suites having the highest $^3He/^4He$ ratios, associated with Iceland and Loihi seamount, have low δD values $< -70‰$ (Fig. 6).

Within individual ocean basins, broad arrays are evident in a diagram of δD vs. $^{87}Sr/^{86}Sr$ (Fig. 7), as well as for other radiogenic systems (Fig. S2). Within the Easter, North Atlantic, and ASP sample suites, basalts with higher δD values appear to trend toward higher $^{87}Sr/^{86}Sr$. Another noteworthy feature is that MORB compositions having the lowest values of δD ($\leq -90‰$) appear to converge toward a common value of $^{87}Sr/^{86}Sr$ near 0.703 (Fig. 7).

4. Origins of δD variability in mantle-derived magmas

D/H ratios have greater variability throughout the solar system than any other isotopic ratio (e.g., Marty and Yokochi, 2006). On Earth, δD values appear to be restricted to a normal distribution between $-100‰$ and $-40‰$ in mantle-derived basalts (Fig. 5; extending to $-30‰$ if conventional analyses are included). We examine some details of the variations within this range to help better constrain Earth's primordial δD value, and to ascertain the processes that might account for deviations from it.

4.1. δD in high $^3He/^4He$ basalts

High and low $^3He/^4He$ basalts span almost the same range of δD (Fig. 5). The δD frequency peak around $-50‰$ observed in high $^3He/^4He$ basalts is best explained by a surface water component that was recycled by subduction and incorporated into the source of mantle plumes near the core–mantle boundary (section 4.1.1). Here the surface water component is assumed to be characterized by δD ~0‰, although values of $-7‰$ or lower may have been present through much of Earth's history (Lécuyer et al., 1998). This peak is dominated by high $^3He/^4He$ basalts from the SEIR and from the Easter hotspot region (Fig. 6; Kingsley et al., 2002; Dixon et al., 2017). The other δD frequency peak around $-75‰$ observed in both high and low $^3He/^4He$ basalts (Fig. 5), and similar to the δD peak in depleted basalts distributed globally, may provide the best characterization of Earth's primordial δD value. It is exemplified by the highest $^3He/^4He$ submarine glasses from Loihi seamount (Fig. 6, section 4.1.2).

4.1.1. Recycled water

Plate tectonic recycling has been recognized for decades as a process of central importance in the geochemical cycle of water (e.g., Ito et al., 1983; Giggenbach, 1992; Lécuyer et al., 1998; Shaw et al., 2008; Dixon et al., 2017). Basalts from subduction zones and back arc basins include high δD values (up to $-20‰$), and early models suggested that residual slabs subducted into the mantle should therefore be deuterium-depleted and subduction zone mantle wedge peridotite should be deuterium-enriched (e.g., Poreda, 1985; Giggenbach, 1992; Shaw et al., 2008). Dixon et al. (2017), however, proposed that rehydration of a slab by higher pressure mineral dehydration may allow some residual slabs to become deuterium-enriched, as also shown by experimental studies of dehydration in mantle minerals (Roskosz et al., 2018). When
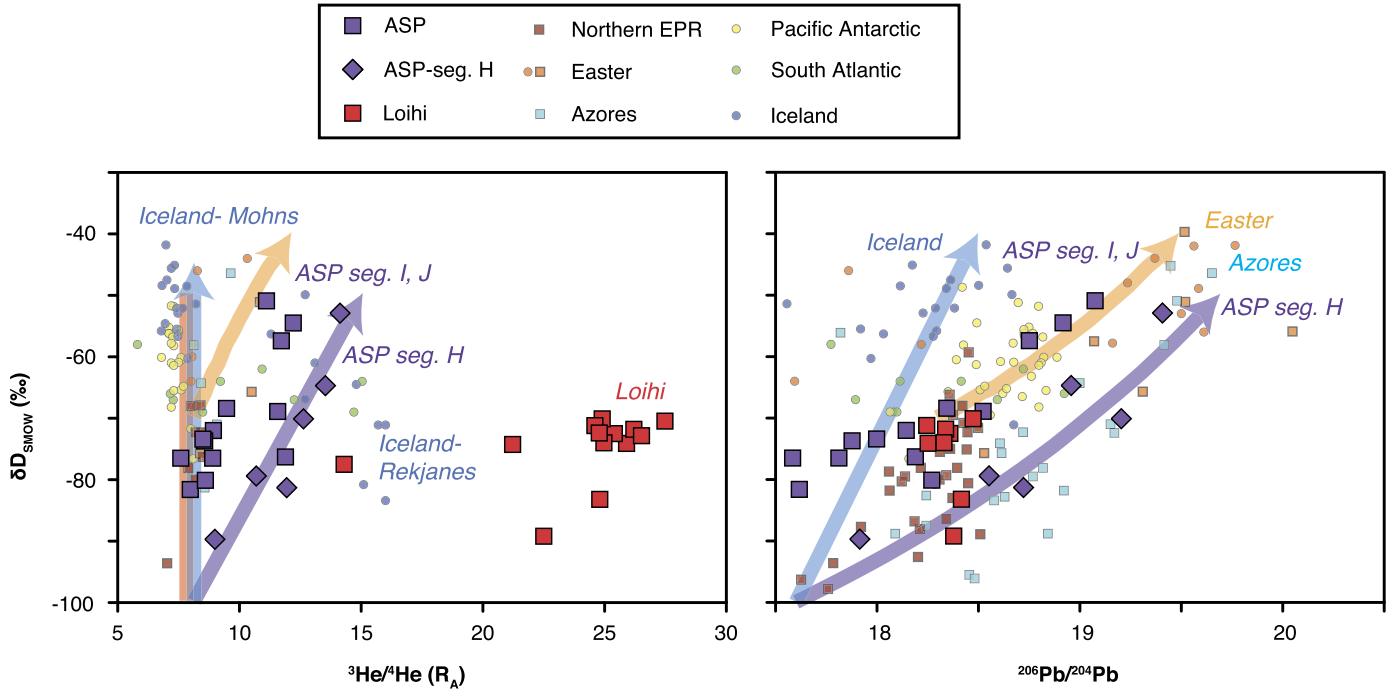
Fig. 6. δD vs. $^3He/^4He$ and $^{206}Pb/^{204}Pb$ in suites of submarine basalts distributed globally. There is a generally positive covariation between δD and $^3He/^4He$ at the ridge segment scale along the Southeast Indian Ridge (ASP) (segment H, I and J; see also Fig. 2). Globally, however, there is no simple trend of δD with helium isotope compositions. Basalts having $^3He/^4He$ <10 R_A extend to the highest δD values, while basalts having the highest $^3He/^4He$ values (from Loihi seamount and also the Reykjanes Ridge) have lower δD of -70 to -90‰. Pb isotopes, as well as other mantle enrichment factors (e.g., La/Sm, K/Ti), show a general positive trend with δD that is best observed within individual sample suites (e.g., ASP segment H). Symbols are the same as Figs. 3 and 4. Colored lines represent model mixing curves chosen to highlight trends in the regional data sets. Details of the mixing calculations are provided in the supplemental material.

subducted into the deep mantle, this D-enriched slab material can be intermixed with other components that comprise the source of mantle plumes. This recycling process can explain high δD values accompanying geochemically enriched signatures in both mid-ocean ridge and ocean island basalts.

Our δD results for the SEIR basalts, and the enriched ASP subgroup (from segments H, I and J), are consistent with the slab rehydration explanation in the Dixon et al. (2017) model. The ASP lavas have higher water contents, δD values up to -50‰, and elevated $^{206}Pb/^{204}Pb$ identical to the C-component of Hanan and Graham (1996). The C-component (interchangeably referred to by Dixon et al., 2017, as PREMA—for PREvalent MAntle—Zindler and Hart, 1986) was postulated by Hanan and Graham (1996) to originate from recycled oceanic crust of predominantly Proterozoic age (600–2000 Ma). The high $^3He/^4He$ ratios, up to 14 R_A, of these samples implies that any such recycled material was mixed with a deep mantle component sampled by the ASP plume. This scenario is consistent with evidence from noble gas and radiogenic isotope systematics (White, 2015) and state-of-the-art simulations of mantle convection (Li et al., 2014) that collectively indicate primordial material and subducted lithosphere can mix in or near the plume generation zones associated with LLSVPs (Large-Low Shear wave Velocity Provinces) at the core–mantle boundary. These recycled materials can subsequently become entrained into a mantle plume. The geochemical arrays for the SEIR basalts are therefore best explained by mixing between ASP plume material (itself a mixture of recycled lithosphere and primordial mantle, see section 4.3), and depleted upper mantle (Fig. 8).

4.1.2. Primordial water

The lower δD mode at Loihi seamount occurs in high $^3He/^4He$ basalts that are geochemically less enriched than those from the ASP and Easter hotspots. Comparable δD values also occur in mod-

erately high $^3He/^4He$ lavas from Iceland (Fig. 6). The lower H_2O/Ce ratios of Loihi basalts relative to other moderately enriched basalts globally seem to suggest a lower water content in the Loihi mantle source (Figs. 3 and 7; Dixon and Clague, 2001), although H_2O/Ce may not be as reliable an indicator of water concentration in OIB source mantle compared to MORB source mantle (e.g., Peslier et al., 2017).

The Dixon et al. (2017) recycling model hypothesizes that the low H_2O and $\delta D = -75$‰ in the Loihi mantle source originates from dehydrated lithosphere of high temperature subducted slabs. This is consistent with the low H_2O/Ce observed in Loihi basalts (Dixon and Clague, 2001). However, such "dry" recycled materials will have a very low proportional contribution of water during mixing with a primordial mantle component (e.g., Marty, 2012). Endmember H_2O concentrations are not well known for such mixing scenarios and this makes quantitative modeling of the mixing very uncertain. Although a contribution of some recycled water to the Loihi mantle source is possible, it seems likely that there is a substantial contribution from primordial mantle. The very high $^3He/^4He$ ratios require the presence of a primordial volatile component, and it must strongly influence, if not dominate, the δD composition of the Loihi source mantle.

Loihi δD values (-75‰) also resemble those for typical MORB mantle (Fig. 5), an observation noted previously by Kyser and O'Neil (1984) and Garcia et al. (1989). Furthermore, typical partial melting is not expected to lead to large differences in δD between basalts and their source mantle (e.g., Bindeman et al., 2012). Therefore, depleted MORB mantle would have lower concentrations of water and ^3He due to their incompatible behavior during melting, but its primordial δD composition should be largely unmodified if the mantle region has not been affected by recycled water.

A primordial δD value near -75‰ is also similar to δD values of chondritic meteorites (e.g., -100 ± 60‰; Robert, 2003; Alexander, 2017). This supports the common argument that the
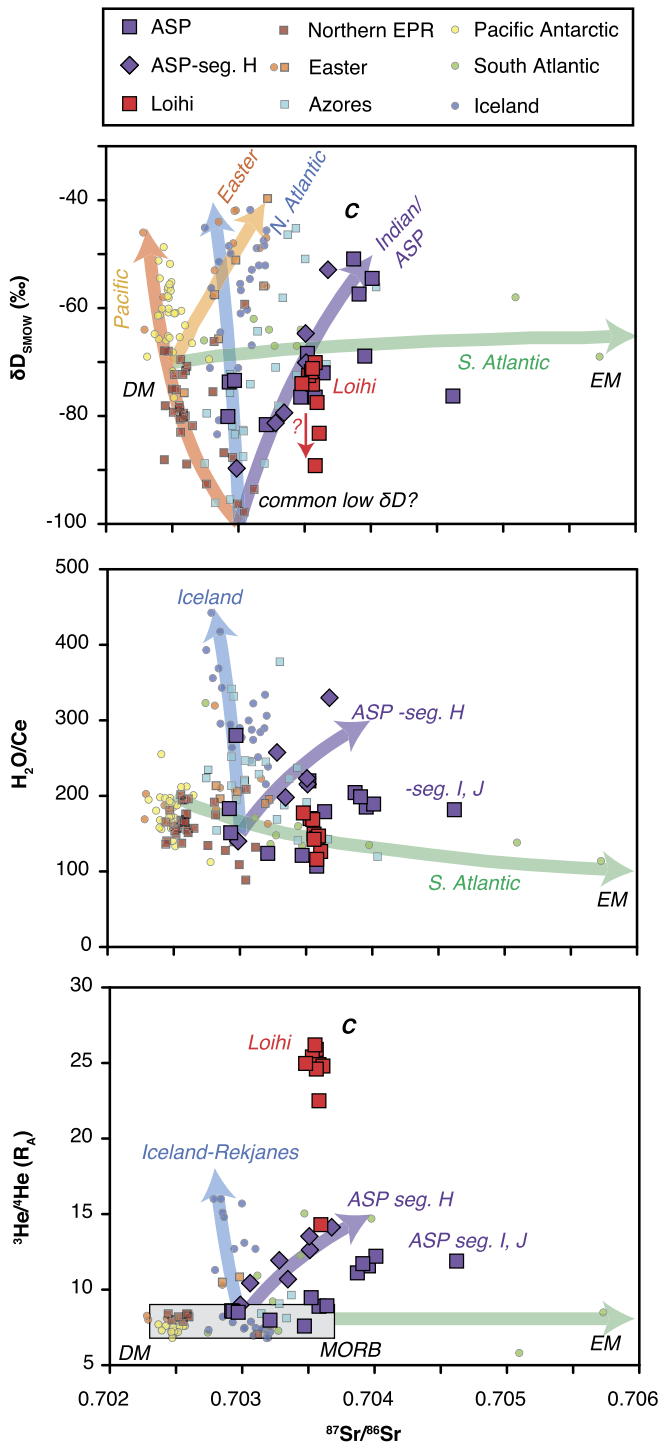
Fig. 7. δD, H_2O/Ce, and $^3He/^4He$ vs. $^{87}Sr/^{86}Sr$ in suites of submarine basalts distributed globally. There are major differences in regional trends in these geochemical tracers with respect to Sr isotopes. Broad differences between major ocean basins, previously described by Dixon et al. (2017), can also be matched to mantle chemical domains: depleted mantle (DM), enriched mantle (EM), and common mantle (C, also referred to as PREMA). Gray box shows the typical MORB range, other symbols are the same as Figs. 3, 4, 6, and 7.

fects of hydrogen dissolution into an early magma ocean when solar nebula gas was still present, along with H isotope fractionation during core formation. The study concluded that a small but significant percentage of hydrogen in the deep Earth has a nebular origin, and that the mantle residue of magma ocean crystallization would have had δD values near $-110\permil$. Given our limited number of δD analyses in Loihi basalts, all of which were collected near the summit, further study of deeper, less degassed submarine basalts from Loihi seamount will likely prove to be important for precisely establishing the primordial value of δD.

The Loihi submarine glass results appear to provide evidence counter to the proposed primordial δD of $<-200\permil$ based on δD of melt inclusions from high $^3He/^4He$ basalts at Baffin Island (Hallis et al., 2015). Melt inclusions may be modified from primary mantle values by diffusive hydrogen exchange through host olivine crystals with water enriched melts (Portnyagin et al., 2008; Gaetani et al., 2012). This process may result in anomalously low δD values (Hauri, 2002; Michael, 2017; Gatti et al., 2018). The Loihi basalt data provide evidence that primordial He isotope signatures in deep mantle plume source regions may be accompanied by δD values near $-75\permil$.
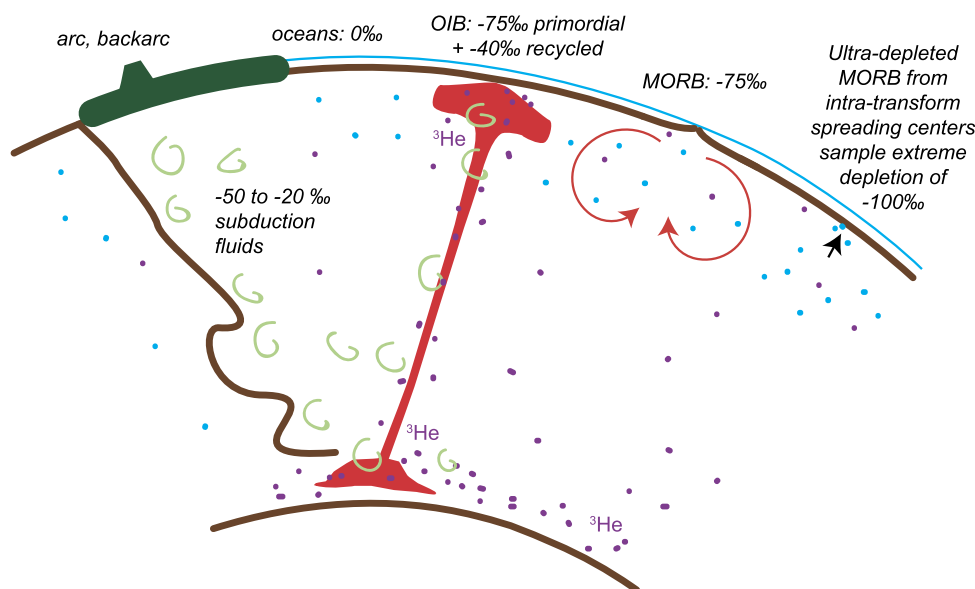
4.2. Depleted δD endmember

The δD values that extend to $-100\permil$ cannot be explained by mixing between primordial water having $\delta D = -75\permil$ and surface water having $\delta D \sim 0\permil$. The low δD limit is similar in all ocean basins (Mid-Atlantic Ridge Azores Plateau, Northern East Pacific Rise, and Southeast Indian Ridge) and it also converges at a common value of $^{87}Sr/^{86}Sr$ near 0.703 (Figs. 3 and 7). One possible explanation is that extreme refinement of the mantle source of the ultra-depleted ridge basalts due to multiple episodes of melt extraction has led to the observed low water concentrations and a lower (fractionated) δD value.

Hydrogen isotope fractionation is usually assumed to be insignificant during the partial melting process (e.g., Kyser and O'Neil, 1984). However, Bindeman et al. (2012) calculated that when melt fractions are low (<1–2%) the melt could have a higher δD value than the source peridotite. This occurs because molecular water that preferentially partitions into the melt is relatively higher in its D/H ratio, while hydrogen that remains in residual anhydrous minerals is relatively lower in D/H. After several percent melting, nearly all the hydrogen will have been incorporated into the melt fraction, leaving little leverage for any D/H fractionation during further melting.

Residual mantle porosity during melting is $<1\%$ based on U-series disequilibria (e.g., Beattie, 1993) and so the partial melting process is a near fractional one and water will be effectively scavenged from the mantle source. Small amounts of hydrogen might be retained in the mantle, however, either as (1) H_2O and OH^- in any residual melt that is not squeezed out during an extraction event, or as (2) minor amounts of hydrogen in nominally anhydrous phases in the mantle (e.g., Bell and Ihinger, 2000). Any residual melts would have the same δD as extracted melts, but H^+ in residual solids can have significantly lower δD (Bell and Ihinger, 2000). Therefore, melts derived from a separate, later melting event involving previously melted mantle, such as the source of ultra-depleted MORB (e.g., Michael and Graham, 2015; Graham et al., 2016), may have the potential to be shifted to lower δD values. More experimental and modeling work is needed to test this idea.

4.3. Mixing of δD between endmembers

Three terrestrial endmember δD compositions are identified here: $\sim 0\permil$ (surface water), $-75\permil$ (primordial water), and $-100\permil$

bulk of Earth's H isotope composition was acquired during the accretion of chondrite-like materials (e.g., Lécuyer et al., 1998; Williams and Hemley, 2001; Marty and Yokochi, 2006; Marty, 2012; Peslier et al., 2017). However, studies of light noble gases (He, Ne) indicate that a solar component may also be present in the deep mantle (Williams and Mukhopadhyay, 2018). A recent planetary modeling study by Wu et al. (2018) considered the ef-

Fig. 8. Schematic diagram of possible mantle sources/processes accounting for the range of δD values in submarine basalt glasses. Relatively high δD values (-50 to $-20‰$) are associated with subduction zone fluids (green swirls, arc, backarc; e.g., Shaw et al., 2008) and with enriched mantle sources such as ocean island basalts (including Amsterdam–St. Paul, Easter; see Fig. 6). Other submarine basalts, including the highest ^{3}He/^{4}He basalts from Loihi seamount, have lower δD near $-75‰$ and may be sampling primordial mantle hydrogen (purple dots) that is dominantly derived from a deep mantle plume source. Very low δD values $<-90‰$ are found in some mid-ocean ridge basalts derived from highly depleted upper mantle domains, sometimes present beneath intra-transform spreading centers. These ultra-depleted MORB glasses may carry a signature of multi-stage melting of their mantle source and isotopic fractionation associated with nominally anhydrous minerals in the residue (light blue dots). Mid-ocean ridge basalts are more commonly melts derived from larger mantle domains that appear to still sample some primordial hydrogen.

(low D/H water, potentially produced by isotopic fractionation during small extents of melting). Mixing proportions in different mantle sources can be estimated from these values.

The highest δD values in the ASP basalt suite suggest that recycled water dominates the signal over primordial water in that region. For example, if the recycled endmember δD is $-20‰$ (the mantle wedge from beneath arc lavas, e.g., Shaw et al., 2008), then the measured values of $-50‰$ in ASP basalts imply that roughly 40% of the H_2O has a recycled origin (assuming a primordial endmember δD of $-75‰$). This argument can extend to He isotopes: the highest ^{3}He/^{4}He ratios in the ASP sample suite are 14 R_A, intermediate between recycled slab compositions (<6 R_A) and higher values characteristic of mantle plume sources beneath Hawaii and Iceland (>30 R_A). Modestly high ^{3}He/^{4}He of 15–20 R_A may result from entrainment and mixing together of primitive and recycled materials (Gonnermann and Mukhopadhyay, 2009).

The depleted endmember δD values that approach $-100‰$ might be caused by $>30\%$ contribution of D/H-depleted nominally anhydrous minerals to residual melt from a MORB source. Mid-ocean ridge basalts that have (La/Sm)$_n < 1$ are offset in δD toward this depleted endmember from primordial values ($-75‰$), suggesting some influence of nominally anhydrous minerals. Many parts of the MORB mantle, however, have δD values that are remarkably similar to $-75‰$ and identical to the δD value of high ^{3}He/^{4}He Loihi samples. This similarity suggests that much of the Earth's mantle still contains a significant component of juvenile water.

5. Conclusions

The lowest δD values in submarine basalts (-90 to $-100‰$) are found in trace element depleted MORB glasses having (La/Sm)$_n < 1$ and roughly similar ^{87}Sr/^{86}Sr = 0.703. This depleted endmember composition potentially results from a multi-stage history of melt extraction (e.g., Michael and Graham, 2015; Graham et al., 2016), during which a small amount of D/H-depleted hydrogen may have been retained within nominally anhydrous minerals in the (residual) mantle that was ultimately melted at a later time.

Submarine basalts with higher δD values are associated with enriched geochemical signatures, such as elevated La/Sm. All submarine basalt glasses with $\delta D > -55‰$ have (La/Sm)$_n > 1$. These enriched, high δD basalts originate from a mantle source that contains a subduction component of water. The correlation of high ^{3}He/^{4}He with δD enrichment in the ASP hotspot-influenced basalts is evidence that the subducted hydrous material was transported into the lower mantle, where it was subsequently entrained into a mantle plume that also tapped a primordial reservoir (Fig. 8).

Most δD values for submarine basalt glasses distributed globally lie in a narrow range of $-75 \pm 12‰$ (1σ, $n = 95$). Submarine basalt glasses having high ^{3}He/^{4}He ratios from Loihi seamount also have $\delta D = -73 \pm 12‰$ and are indistinguishable from the global average. In contrast to the dominantly recycled δD signature that trends to $-50‰$ in ASP hotspot basalts having high ^{3}He/^{4}He ratios, the δD values from Loihi seamount arguably provide a current best estimate for Earth's primordial δD. Some high ^{3}He/^{4}He mantle source regions appear to still contain a significant component of their primordial water.

Appendix A. Supplementary material

Supplementary material related to this article can be found online at https://doi.org/10.1016/j.epsl.2018.12.012.

References

Alexander, C.M.O., 2017. The origin of inner Solar System water. Philos. Trans. R. Soc. Lond. A 375. https://doi.org/10.1098/rsta.2015.0384.

Allègre, C.J., Staudacher, T., Sarda, P., Kurz, M., 1983. Constraints on evolution of Earth's mantle from rare gas systematics. Nature 303, 762–766. https://doi.org/10.1038/303762a0.

Aubaud, C., Hauri, E.H., Hirschmann, M.M., 2004. Hydrogen partition coefficients between nominally anhydrous mantle minerals and basaltic melts. Geophys. Res. Lett. 31, L20611. https://doi.org/10.1029/2004GL021341.

Beattie, P., 1993. Uranium–thorium disequilibria and partitioning on melting of garnet peridotite. Nature 363, 63–65. https://doi.org/10.1038/363063a0.

Bell, D.R., Ihinger, P.D., 2000. The isotopic composition of hydrogen in nominally anhydrous mantle minerals. Geochim. Cosmochim. Acta 64, 2109–2118. https://doi.org/10.1016/S0016-7037(99)00440-8.

Bindeman, I.N., Kamenetsky, V.S., Palandri, J., Vennemann, T., 2012. Hydrogen and oxygen isotope behaviors during variable degrees of upper mantle melting: example from the basaltic glasses from Macquarie Island. Chem. Geol. 310–311, 126–136. https://doi.org/10.1016/j.chemgeo.2012.03.031.

Clog, M., Aubaud, C., Cartigny, P., Dosso, L., 2013. The hydrogen isotopic composition and water content of southern Pacific MORB: a reassessment of the D/H ratio of the depleted mantle reservoir. Earth Planet. Sci. Lett. 381, 156–165. https://doi.org/10.1016/j.epsl.2013.08.043.

Clog, M., Cartigny, P., Aubaud, C., 2012. Experimental evidence for interaction of water vapor and platinum crucibles at high temperatures: implications for volatiles from igneous rocks and minerals. Geochim. Cosmochim. Acta 83, 125–137. https://doi.org/10.1016/j.gca.2011.12.020.

Craig, H., Lupton, J.E., 1976. Primordial neon, helium, and hydrogen in oceanic basalts. Earth Planet. Sci. Lett. 31, 369–385. https://doi.org/10.1016/0012-821X(76)90118-7.

De Hoog, J.C.M., Taylor, B.E., Van Bergen, M.J., 2009. Hydrogen-isotope systematics in degassing basaltic magma and application to Indonesian arc basalts. Chem. Geol. 266, 256–266. https://doi.org/10.1016/j.chemgeo.2009.06.010.

Dixon, J.E., Bindeman, I.N., Kingsley, R.H., Simons, K.K., Le Roux, P.J., Hajewski, T.R., Swart, P., Langmuir, C.H., Ryan, J.G., Walowski, K.J., Wada, I., Wallace, P.J., 2017. Light stable isotopic compositions of enriched mantle sources: resolving the dehydration paradox. Geochem. Geophys. Geosyst. 18, 1–39. https://doi.org/10.1002/2016GC006743.

Dixon, J.E., Clague, D.A., 2001. Volatiles in basaltic glasses from Loihi seamount, Hawaii: evidence for a relatively dry plume component. J. Petrol. 42, 627–654. https://doi.org/10.1093/petrology/42.3.627.

Douglas-Priebe, L.M., 1998. Geochemical and Petrogenetic Effects of the Interaction of the Southeast Indian Ridge and the Amsterdam–Saint Paul Hotspot. M.S. thesis. Oregon State University, Corvallis. 132 p.

Friedman, I., 1967. Water and deuterium in pumice from the 1959–1960 eruption of Kilauea Volcano, Hawaii. U.S. Geological Survey Professional Paper 575-B, 120–127.

Gaetani, G.A., O'Leary, J.A., Shimizu, N., Bucholz, C.E., Newville, M., 2012. Rapid reequilibration of H_2O and oxygen fugacity in olivine-hosted melt inclusions. Geology 40, 915–918. https://doi.org/10.1130/G32992.1.

Garcia, M.O., Jorgenson, B.A., Mahoney, J.J., 1993. An evaluation of temporal geochemical evolution of Loihi summit lavas: results from *Alvin* submersible dives. J. Geophys. Res. 98, 537–550. https://doi.org/10.1029/92JB01707.

Garcia, M.O., Muenow, D.W., Aggrey, K.E., O'Neil, J.R., 1989. Major element, volatile, and stable isotope geochemistry of Hawaiian submarine tholeiitic glasses. J. Geophys. Res. 94, 10525–10538. https://doi.org/10.1029/JB094iB08p10525.

Garcia, M.O., Rubin, K.H., Norman, M.D., Rhodes, J.M., Graham, D.W., Muenow, D., Spencer, K., 1998. Petrology and geochronology of basalt breccia from the 1996 earthquake swarm of Loihi seamount, Hawaii: magmatic history of its 1996 eruption. Bull. Volcanol. 59, 577–592. https://doi.org/10.1007/s004450050211.

Gatti, E., Bucholz, C., Guan, Y., Zhang, Y., Gaetani, G., Eiler, J., 2018. δD variations in olivine-hosted melt inclusions due to post-entrapment processes: a case study from Baffin Island picrites. In: Goldschmidt 2018 Abstracts, p. 798.

Giggenbach, W.F., 1992. Isotopic shifts in waters from geothermal and volcanic systems along convergent plate boundaries and their origin. Earth Planet. Sci. Lett. 113, 495–510. https://doi.org/10.1016/0012-821X(92)90127-H.

Gonnermann, H.M., Mukhopadhyay, S., 2009. Preserving noble gases in a convecting mantle. Nature 459, 560–563. https://doi.org/10.1038/nature08018.

Graham, D.W., Hanan, B.B., Hémond, C., Blichert-Toft, J., Albarède, F., 2014. Helium isotopic textures in Earth's upper mantle. Geochem. Geophys. Geosyst. 15, 2048–2074. https://doi.org/10.1002/2014GC005264.

Graham, D.W., Jenkins, W.J., Kurz, M.D., Batiza, R., 1987. Helium isotope disequilibrium and geochronology of glassy submarine basalts. Nature 326, 384–386. https://doi.org/10.1038/326384a0.

Graham, D.W., Johnson, K., Douglas Priebe, L., Lupton, J.E., 1999. Hotspot–ridge interaction along the Southeast Indian Ridge near Amsterdam and St. Paul islands: helium isotope evidence. Earth Planet. Sci. Lett. 167, 297–310. https://doi.org/10.1016/S0012-821X(99)00030-8.

Graham, D.W., Michael, P.J., Shea, T., 2016. Extreme incompatibility of helium during mantle melting: evidence from undegassed mid-ocean ridge basalts. Earth Planet. Sci. Lett. 454, 192–202. https://doi.org/10.1016/j.epsl.2016.09.016.

Hallis, L.J., Huss, G.R., Nagashima, K., Taylor, G.J., Halldórsson, S.A., Hilton, D.R., Mottl, M.J., Meech, K.J., 2015. Evidence for primordial water in Earth's deep mantle. Science 350, 795–797. https://doi.org/10.1126/science.aac4834.

Hanan, B.B., Graham, D.W., 1996. Lead and helium isotope evidence from Oceanic Basalts for a common deep source of mantle plumes. Science 272, 991–995. https://doi.org/10.1126/science.272.5264.991.

Hart, S.R., 1984. A large-scale isotope anomaly in the Southern Hemisphere mantle. Nature 309, 753–757. https://doi.org/10.1038/309753a0.

Hauri, E.H., 2002. SIMS analysis of volatiles in silicate glasses, 2: isotopes and abundances in Hawaiian melt inclusions. Chem. Geol. 183, 115–141. https://doi.org/10.1016/S0009-2541(01)00374-6.

Hirschmann, M.M., 2006. Water, melting, and the deep Earth H_2O cycle. Annu. Rev. Earth Planet. Sci. 34, 629–653. https://doi.org/10.1146/annurev.earth.34.031405.125211.

Honda, M., McDougall, I., Patterson, D., Doulgeris, A., Clague, D.A., 1993. Noble gases in submarine pillow basalt glasses from Loihi and Kilauea, Hawaii: a solar component in the Earth. Geochim. Cosmochim. Acta 57, 859–874. https://doi.org/10.1016/0016-7037(93)90174-U.

Ito, E., Harris, D.M., Anderson, A.T. Jr., 1983. Alteration of oceanic crust and geologic cycling of chlorine and water. Geochim. Cosmochim. Acta 47, 1613–1624. https://doi.org/10.1016/0016-7037(83)90188-6.

Johnson, K.T.M., Graham, D.W., Rubin, K.H., Nicolaysen, K., Scheirer, D.S., Forsyth, D.W., Baker, E.T., Douglas-Priebe, L.M., 2000. Boomerang seamount: the active expression of the Amsterdam–St. Paul hotspot, Southeast Indian Ridge. Earth Planet. Sci. Lett. 183, 245–259. https://doi.org/10.1016/S0012-821X(00)00279-X.

Kent, A.J., Clague, D.A., Honda, M., Stolper, E.M., Hutcheon, I., Norman, M.D., 1999. Widespread assimilation of a seawater-derived component at Loihi Seamount, Hawaii. Geochim. Cosmochim. Acta 63, 2749–2761. https://doi.org/10.1016/S0016-7037(99)00215-X.

Kingsley, R.H., Schilling, J.-G., Dixon, J.E., Swart, P., Poreda, R., Simons, K., 2002. D/H ratios in basalt glasses from the Salas y Gomez mantle plume interacting with the East Pacific Rise: water from old D-rich recycled crust or primordial water from the lower mantle? Geochem. Geophys. Geosyst. 3, 1–26. https://doi.org/10.1029/2001GC000199.

Kurz, M.D., Jenkins, W.J., Hart, S.R., 1982. Helium isotopic systematics of oceanic islands and mantle heterogeneity. Nature 297, 43–46. https://doi.org/10.1038/297043a0.

Kurz, M.D., Jenkins, W.J., Hart, S.R., Clague, D., 1983. Helium isotopic variations in volcanic rocks from Loihi Seamount and the Island of Hawaii. Earth Planet. Sci. Lett. 66, 388–406. https://doi.org/10.1016/0012-821X(83)90154-1.

Kyser, T.K., O'Neil, J.R., 1984. Hydrogen isotope systematics of submarine basalts. Geochim. Cosmochim. Acta 48, 2123–2133. https://doi.org/10.1016/0016-7037(84)90392-2.

Lécuyer, C., Gillet, P., Robert, F., 1998. The hydrogen isotope composition of seawater and the global water cycle. Chem. Geol. 145, 249–261. https://doi.org/10.1016/S0009-2541(97)00146-0.

Li, M., McNamara, A.K., Garnero, E.J., 2014. Chemical complexity of hotspots caused by cycling oceanic crust through mantle reservoirs. Nat. Geosci. 7, 366–370. https://doi.org/10.1038/ngeo2120.

Loewen, M.W., Kent, A.J., 2012. Sources of elemental fractionation and uncertainty during the analysis of semi-volatile metals in silicate glasses using LA-ICP-MS. J. Anal. At. Spectrom. 27, 1502–1508. https://doi.org/10.1039/c2ja30075c.

Martin, E., Bindeman, I.N., Balan, E., Palandri, J., Seligman, A., Villemant, B., 2017. Hydrogen isotope determination by TC/EA technique in application to volcanic glass as a window into secondary hydration. J. Volcanol. Geotherm. Res. 348, 49–61. https://doi.org/10.1016/j.jvolgeores.2017.10.013.

Marty, B., 2012. The origins and concentrations of water, carbon, nitrogen and noble gases on Earth. Earth Planet. Sci. Lett. 313–314, 56–66. https://doi.org/10.1016/j.epsl.2011.10.040.

Marty, B., Yokochi, R., 2006. Water in the early Earth. Rev. Mineral. Geochem. 62, 421–450. https://doi.org/10.2138/rmg.2006.62.18.

McGovern, J., Schubert, G., 1989. Thermal evolution of the Earth: effects of volatile exchange between atmosphere and interior. Earth Planet. Sci. Lett. 96, 27–37. https://doi.org/10.1016/0012-821X(89)90121-0.

Michael, P.J., 2017. Low D/H in Baffin Island melt inclusions: primordial water or diffusive hydration of inclusions? In: Goldschmidt 2017 Abstracts, p. 2712.

Michael, P.J., Cornell, W.C., 1998. Influence of spreading rate and magma supply on crystallization and assimilation beneath mid-ocean ridges: evidence from chlorine and major element chemistry of mid-ocean ridge basalts. J. Geophys. Res. 103, 18325–18356. https://doi.org/10.1029/98JB00791.

Michael, P.J., Graham, D.W., 2015. The behavior and concentration of CO_2 in the suboceanic mantle: inferences from undegassed ocean ridge and ocean island basalts. Lithos 236–237, 338–351. https://doi.org/10.1016/j.lithos.2015.08.020.

Moore, J.G., Clague, D.A., Normark, W.R., 1982. Diverse basalt types from Loihi seamount, Hawaii. Geology 10, 88–92. https://doi.org/10.1130/0091-7613(1982)10<88:DBTFLS>2.0.CO;2.

Mukhopadhyay, S., 2012. Early differentiation and volatile accretion recorded in deep-mantle neon and xenon. Nature 486, 101–104. https://doi.org/10.1038/nature11141.

Newman, S., Lowenstern, J.B., 2002. VolatileCalc: a silicate melt–H_2O–CO_2 solution model written in Visual Basic for excel. Comput. Geosci. 28, 597–604. https://doi.org/10.1016/S0098-3004(01)00081-4.

Nicolaysen, K.P., Frey, F.A., Mahoney, J.J., Johnson, K.T.M., Graham, D.W., 2007. Influence of the Amsterdam/St. Paul hot spot along the Southeast Indian Ridge between 77° and 88°E: correlations of Sr, Nd, Pb, and He isotopic variations with ridge segmentation. Geochem. Geophys. Geosyst. 8, 1–24. https://doi.org/10.1029/2006GC001540.

Parai, R., Mukhopadhyay, S., 2012. How large is the subducted water flux? New constraints on mantle regassing rates. Earth Planet. Sci. Lett. 317–318, 396–406. https://doi.org/10.1016/j.epsl.2011.11.024.

Peslier, A.H., Schönbächler, M., Busemann, H., Karato, S.I., 2017. Water in the Earth's interior: distribution and origin. Space Sci. Rev. 212, 743–810. https://doi.org/10.1007/s11214-017-0387-z.

Pietruszka, A.J., Keyes, M.J., Duncan, J.A., Hauri, E.H., Carlson, R.W., Garcia, M.O., 2011. Excesses of seawater-derived ^{234}U in volcanic glasses from Loihi Seamount due to crustal contamination. Earth Planet. Sci. Lett. 304, 280–289. https://doi.org/10.1016/j.epsl.2011.02.018.

Poreda, R., 1985. Helium-3 and deuterium in back-arc basalts: Lau Basin and the Mariana Trough. Earth Planet. Sci. Lett. 73, 244–254. https://doi.org/10.1016/0012-821X(85)90073-1.

Poreda, R., Schilling, J.G., Craig, H., 1986. Helium and hydrogen isotopes in ocean-ridge basalts north and south of Iceland. Earth Planet. Sci. Lett. 78, 1–17. https://doi.org/10.1016/0012-821X(86)90168-8.

Poreda, R.J., Schilling, J.G., Craig, H., 1993. Helium isotope ratios in Easter microplate basalts. Earth Planet. Sci. Lett. 119, 319–329. https://doi.org/10.1016/0012-821X(93)90141-U.

Portnyagin, M., Almeev, R., Matveev, S., Holtz, F., 2008. Experimental evidence for rapid water exchange between melt inclusions in olivine and host magma. Earth Planet. Sci. Lett. 272, 541–552. https://doi.org/10.1016/j.epsl.2008.05.020.

Qi, H., Colen, T.B., Gehre, M., Vennermann, T.W., Brand, W.A., Geilmann, H., Olack, G., Bindeman, I.N., Palandri, J., Huang, L., Longstraffe, F.J., 2017. New biotite and muscovite isotopic reference materials, USGS57 and USGS58, for δ^2H measurements—a replacement for NBS 30. Chem. Geol. 467, 89–99. https://doi.org/10.1016/j.chemgeo.2017.07.027.

Qi, H., Coplen, T.B., Olack, G.A., Vennemann, T.W., 2014. Caution on the use of NBS 30 biotite for hydrogen-isotope measurements with on-line high-temperature conversion systems. Rapid Commun. Mass Spectrom. 28, 1987–1994. https://doi.org/10.1002/rcm.6983.

Qi, H., Gröning, M., Coplen, T.B., Buck, B., Mroczkowski, S.J., Brand, W.A., Geilmann, H., Gehre, M., 2010. Novel silver-tubing method for quantitative introduction of water into high-temperature conversion systems for stable hydrogen and oxygen isotopic measurements. Rapid Commun. Mass Spectrom. 24, 1821–1827. https://doi.org/10.1002/rcm.4559.

Roskosz, M., Deloule, E., Ingrin, J., Depecker, C., Laporte, D., Merkel, S., Remusat, L., Leroux, H., 2018. Kinetic D/H fractionation during hydration and dehydration of silicate glasses, melts and nominally anhydrous minerals. Geochim. Cosmochim. Acta 233, 14–32. https://doi.org/10.1016/j.gca.2018.04.027.

Rison, W., Craig, H., 1983. Helium isotopes and mantle volatiles in Loihi Seamount and Hawaiian Island basalts and xenoliths. Earth Planet. Sci. Lett. 66, 407–426. https://doi.org/10.1016/0012-821X(83)90155-3.

Robert, F., 2003. The D/H ratio in chondrites. Space Sci. Rev. 106, 87–101. https://doi.org/10.1023/A:1024629402715.

Sharp, Z.D., Atudorei, V., Durakiewicz, T., 2001. A rapid method for determination of hydrogen and oxygen isotope ratios from water and hydrous minerals. Chem. Geol. 178, 197–210. https://doi.org/10.1016/S0009-2541(01)00262-5.

Shaw, A.M., Hauri, E.H., Fischer, T.P., Hilton, D.R., Kelley, K.A., 2008. Hydrogen isotopes in Mariana arc melt inclusions: implications for subduction dehydration and the deep-Earth water cycle. Earth Planet. Sci. Lett. 275, 138–145. https://doi.org/10.1016/j.epsl.2008.08.015.

White, W.M., 2015. Isotopes, DUPAL, LLSVPs, and Anekantavada. Chem. Geol. 419, 10–28. https://doi.org/10.1016/j.chemgeo.2015.09.026.

Williams, Q., Hemley, R.J., 2001. Hydrogen in the deep Earth. Annu. Rev. Earth Planet. Sci. 29, 365–418. https://doi.org/10.1146/annurev.earth.29.1.365.

Williams, Q., Mukhopadhyay, S., 2018. Capture of nebular gasses during Earth's accretion is preserved in deep-mantle neon. Nature. https://doi.org/10.1038/s41586-018-0771-1. In press.

Wu, J., Desch, S.J., Schaefer, L., Elkins-Tanton, L.T., Pahlevan, K., Buseck, P.R., 2018. Origin of Earth's water: chondritic inheritance plus nebular ingassing and storage of hydrogen in the core. J. Geophys. Res. 123, 2691–2712. https://doi.org/10.1029/2018JE005698.

Zindler, A., Hart, S., 1986. Chemical geodynamics. Annu. Rev. Earth Planet. Sci. 14, 493–571. https://doi.org/10.1146/annurev.ea.14.050186.002425.